DEPARTMENT OF CIVIL ENGINEERING
AALBORG UNIVERSITY

Theory and Analysis of JolTech’s GyroPTO

Adi Kurniawan
Jens Peter Kofoed
Morten Bech Kramer

Carried out under contract for:

JolTech ApS

Co-funded by

eUDP

DCE Contract Report No. 194

Aalborg University
Department of Civil Engineering
Wave Energy Research Group

DCE Contract Report No. 194

Theory and Analysis of JolTech's GyroPTO

by

Adi Kurniawan
Jens Peter Kofoed
Morten Bech Kramer

April 2018

© Aalborg University

Scientific Publications at the Department of Civil Engineering

Technical Reports are published for timely dissemination of research results and scientific work carried out at the Department of Civil Engineering (DCE) at Aalborg University. This medium allows publication of more detailed explanations and results than typically allowed in scientific journals.

Technical Memoranda are produced to enable the preliminary dissemination of scientific work by the personnel of the DCE where such release is deemed to be appropriate. Documents of this kind may be incomplete or temporary versions of papers—or part of continuing work. This should be kept in mind when references are given to publications of this kind.

Contract Reports are produced to report scientific work carried out under contract. Publications of this kind contain confidential matter and are reserved for the sponsors and the DCE. Therefore, Contract Reports are generally not available for public circulation.

Lecture Notes contain material produced by the lecturers at the DCE for educational purposes. This may be scientific notes, lecture books, example problems or manuals for laboratory work, or computer programs developed at the DCE.

Theses are monograms or collections of papers published to report the scientific work carried out at the DCE to obtain a degree as either PhD or Doctor of Technology. The thesis is publicly available after the defence of the degree.

Latest News is published to enable rapid communication of information about scientific work carried out at the DCE. This includes the status of research projects, developments in the laboratories, information about collaborative work and recent research results.

Published 2018 by
Aalborg University
Department of Civil Engineering
Thomas Manns Vej 23
DK-9220 Aalborg Ø, Denmark

Printed in Aalborg at Aalborg University

DCE Contract Report No. 194

1 Introduction

This report summarizes the work done by Aalborg University (AAU) for the project "Gyro electric energy converter theory and analysis" (Olsen, 2015). The project's objective is to build a theoretical knowledge about gyro electric energy conversion systems, particularly for use in connection with wave energy.

The JolTech wave energy converter was first conceived in 2010. The Gyroscopic power take-off (GyroPTO) has the operational principle similar to the gyroscopic hand wrist exerciser (Gulick and O'Reilly, 2000). The system is made up of a spinning flywheel with its spin axis in rolling contact to a ring (figure 1). In a synchronized state, the rotational speed of the ring is equal to the wave angular frequency. In this state, the flywheel is running at almost constant speed, so the generated power from the generator becomes constant as well, making the need for additional power electronics unnecessary before the power can be supplied to the grid.

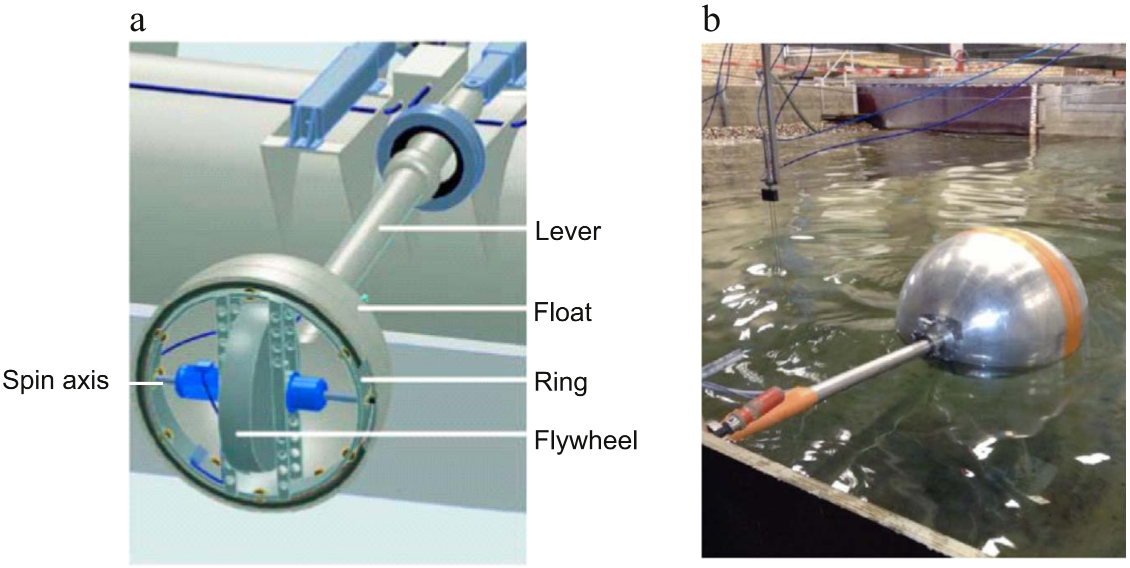

Figure 1: (a) Schematic view and (b) scaled model of the GyroPTO device, from Zhang et al. (2017).

In a previous study (Nielsen et al., 2015), it is shown that the GyroPTO device performs well in monochromatic waves, but synchronization of the device is easily lost in irregular waves. Results from scaled model tests support these findings, where a capture width ratio of approximately 33% was measured in regular waves. However, a completely different picture was obtained from irregular waves: the performance was generally very unstable, and the system hardly absorbed any power (Kramer and Kofoed, 2016; Kramer et al., 2015).

To improve the performance of the device in irregular seas, a magnetic coupling mechanism has been proposed between the spin axis and the flywheel, which acts as a linear viscous damping mechanism on the flywheel. The idea of this mechanism is to reduce fluctuation of the spinning velocity of the flywheel, and hence stabilize the synchronization of the GyroPTO device. The performance of this mechanism is the subject of the following section.

2 Performance at Nissum Bredning

The performance of the coupling mechanism has been investigated theoretically by (Zhang et al., 2017). The theoretical modelling of the GyroPTO was carried out using analytical rigid body dynamics, and linear wave theory was applied to calculate the hydrodynamic moments acting on the float. A detailed description of the model, including the magnetic coupling mechanism, is given in the paper. The paper has been reviewed in connection to the writing of the current report, and a major error in the numerical code was found and corrected. The numerical results in the paper by Zhang et al. (2017) are therefore incorrect, and so are the conclusions. In the following, new simulations with the corrected code are included.

To have an idea of how well the device performs in typical wave climates, the performance of GyroPTO in Nissum Bredning is investigated numerically. The numerical model is implemented in MATLAB, and two MATLAB codes, `Nonlinear_14StateVector.m` and `WaveExcitationForce.m`, constitute the basis of the analysis. The first code evaluates quantities such as the angular velocities and power output of the device. Among the input variables are the generator gain c_g and the damping coefficient c_c. The code takes as input pre-calculated time series of the excitation moments (as `.mat` files), which are generated by `WaveExcitationForce.m` based on the JONSWAP spectrum.

The wave scatter diagram at Nissum Bredning is provided by Nielsen and Pontes (2010, page 28), where the sea states are described in terms of the significant wave height H_s and peak period T_p (see figure 2). The mean wave power resource at this location is 0.22 kW/m.

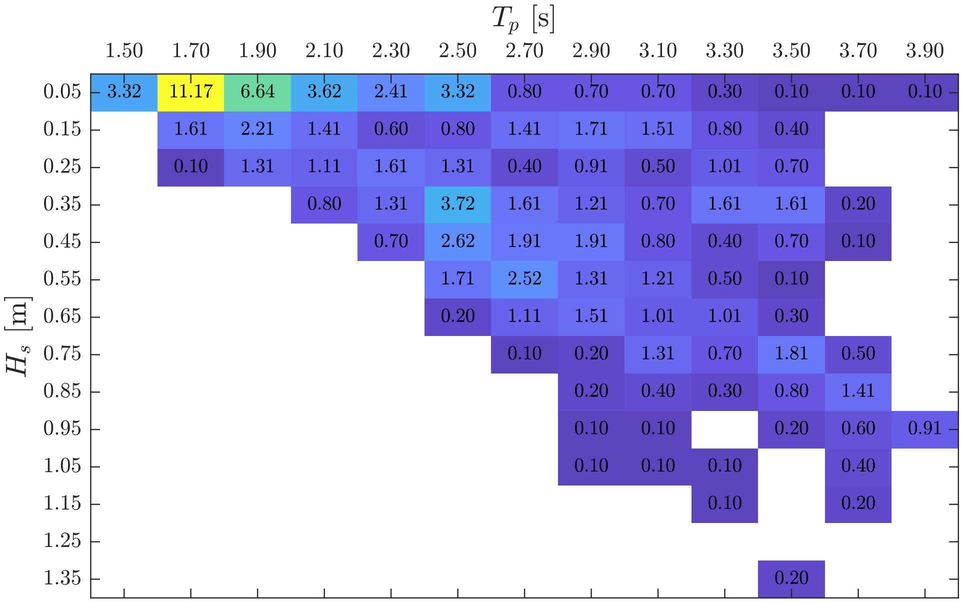

H_s [m] \ T_p [s]	1.50	1.70	1.90	2.10	2.30	2.50	2.70	2.90	3.10	3.30	3.50	3.70	3.90
0.05	3.32	11.17	6.64	3.62	2.41	3.32	0.80	0.70	0.70	0.30	0.10	0.10	0.10
0.15		1.61	2.21	1.41	0.60	0.80	1.41	1.71	1.51	0.80	0.40		
0.25		0.10	1.31	1.11	1.61	1.31	0.40	0.91	0.50	1.01	0.70		
0.35				0.80	1.31	3.72	1.61	1.21	0.70	1.61	1.61	0.20	
0.45					0.70	2.62	1.91	1.91	0.80	0.40	0.70	0.10	
0.55						1.71	2.52	1.31	1.21	0.50	0.10		
0.65						0.20	1.11	1.51	1.01	1.01	0.30		
0.75							0.10	0.20	1.31	0.70	1.81	0.50	
0.85								0.20	0.40	0.30	0.80	1.41	
0.95								0.10	0.10		0.20	0.60	0.91
1.05								0.10	0.10	0.10		0.40	
1.15										0.10		0.20	
1.25													
1.35											0.20		

Figure 2: Wave scatter diagram at Nissum Bredning (Nielsen and Pontes, 2010), showing the probability of occurence in %.

The device at Nissum Bredning was designed to have a diameter of 1.5 m. The simulation is performed at lab scale, where the scale of the device at Nissum Bredning relative to the lab scale is given as 2.57 (Kramer et al., 2015, page 9). Therefore, the corresponding H_s and T_p at lab scale are obtained by dividing the Nissum-scale H_s and T_p by 2.57 and $\sqrt{2.57}$, respectively. Time series of excitation moments (at lab scale), each 2000-second long, are generated and stored for each of the sea states having probability of occurence greater than zero. The peakedness factor $\gamma = 3.3$ is used for the JONSWAP wave spectrum.

Three cases are considered, depending on how the damping coefficient c_c and generator gain c_g are selected for each sea state. In all cases, synchronization and hence a stable power output have not been found.

Case 1 uses constant values of (lab-scale) damping coefficient $c_c = c_{c0} = 0.052$ Nms and generator gain $c_g = c_{g0} = 3.5 \times 10^{-4}$ Nms for all sea states. These were the base values used by Zhang et al. (2017). The instantaneous captured power as a function of time, for each sea

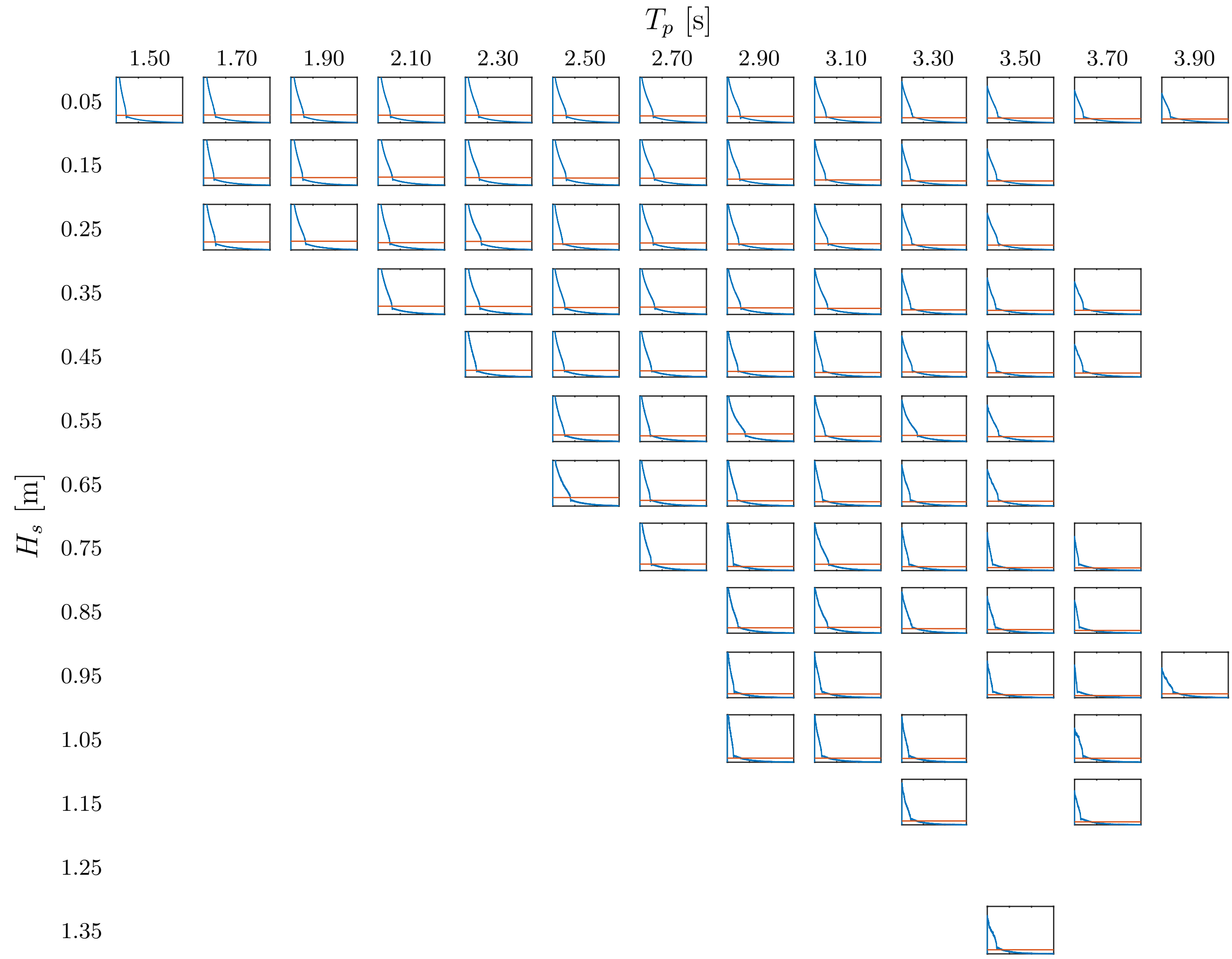

Figure 3: Instantaneous captured power for case 1, $c_c = 0.052$ Nms and $c_g = 3.5 \times 10^{-4}$ Nms. The extents of the horizontal and vertical axes of each plot are 3000 seconds and 50 W.

state, is shown in figure 3. As seen from figure 3, the power in case 1 declines quite rapidly to zero for all sea states.

For case 2, $c_c = 0.052$ Nms is kept constant for all sea states, while c_g is optimized to maximize the mean power output for each sea state. The MATLAB function `fminbnd` is used for this purpose and so the problem is cast into a minimization problem with the objective of minimizing the inverse of the mean power. The values of c_g are kept within the interval $0.5\, c_{g0} < c_g < 2\, c_{g0}$. The optimized c_g values are shown in figure 4. As seen from figure 5, the power declines quite rapidly to zero in case 2.

For case 3, both c_c and c_g are optimized for each sea state. The MATLAB function `fminsearch` is used, and c_c and c_g are kept within the intervals $0.6\, c_{c0} < c_c < 1.4\, c_{c0}$ and $0.5\, c_{g0} < c_g < 2\, c_{g0}$, while $c_c = c_{c0}$ and $c_g = c_{g0}$ are used as the starting values. Since it is not possible to specify the lower and upper bounds directly as arguments in `fminsearch`, the bounds are enforced by letting the mean power output be very small whenever the bounds are exceeded. The optimized c_c and c_g values are shown in figure 6. As seen from figure 7, the power also declines quite rapidly to zero in case 3.

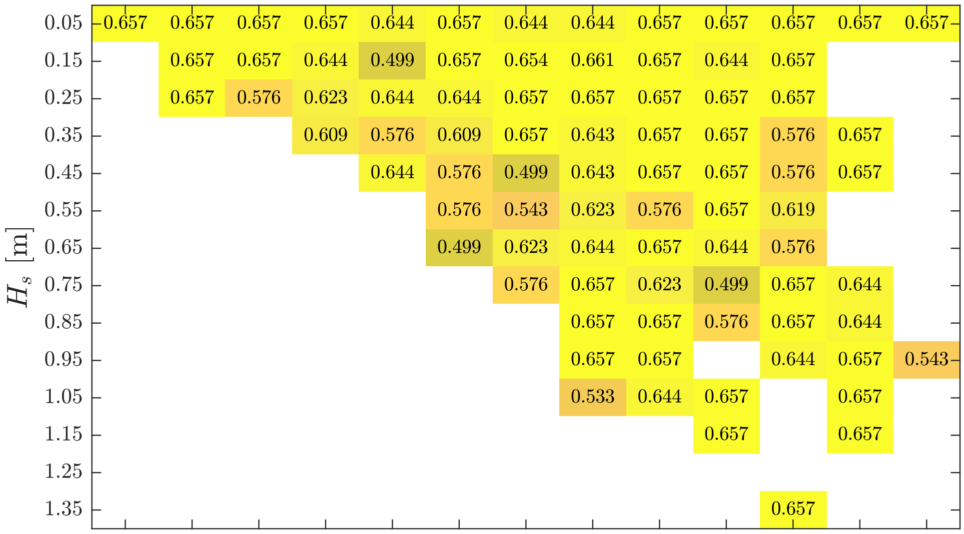

H_s [m]													
0.05	0.657	0.657	0.657	0.657	0.644	0.657	0.644	0.644	0.657	0.657	0.657	0.657	0.657
0.15		0.657	0.657	0.644	0.499	0.657	0.654	0.661	0.657	0.644	0.657		
0.25		0.657	0.576	0.623	0.644	0.644	0.657	0.657	0.657	0.657	0.657		
0.35				0.609	0.576	0.609	0.657	0.643	0.657	0.657	0.576	0.657	
0.45					0.644	0.576	0.499	0.643	0.657	0.657	0.576	0.657	
0.55						0.576	0.543	0.623	0.576	0.657	0.619		
0.65						0.499	0.623	0.644	0.657	0.644	0.576		
0.75							0.576	0.657	0.623	0.499	0.657	0.644	
0.85								0.657	0.657	0.576	0.657	0.644	
0.95								0.657	0.657		0.644	0.657	0.543
1.05								0.533	0.644	0.657		0.657	
1.15										0.657		0.657	
1.25													
1.35											0.657		

Figure 4: Optimized c_g matrix (in 10^{-3} Nms) for case 2, $c_c = 0.052$ Nms.

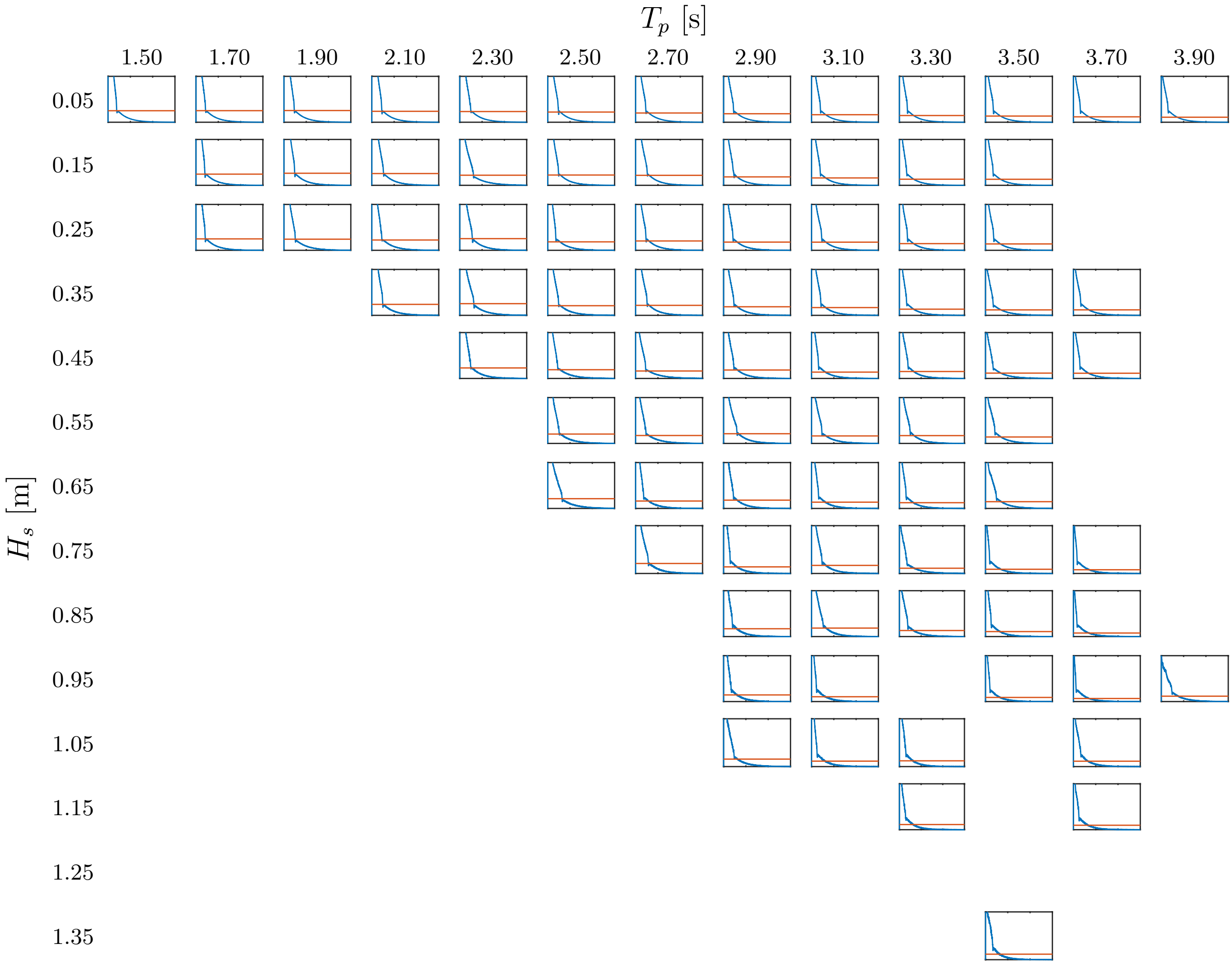

Figure 5: Instantaneous captured power for case 2, $c_c = 0.052$ Nms and c_g optimized.

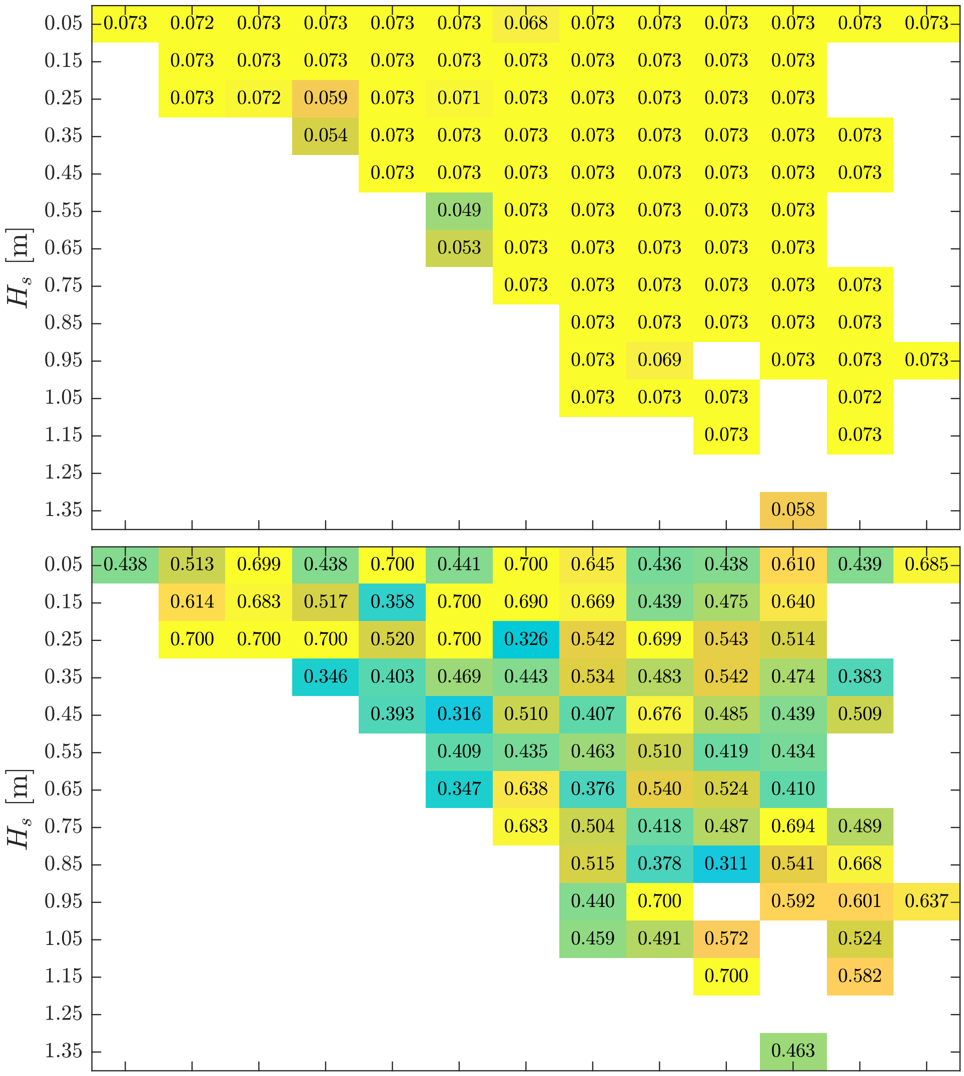

H_s [m]													
0.05	0.073	0.072	0.073	0.073	0.073	0.073	0.068	0.073	0.073	0.073	0.073	0.073	0.073
0.15		0.073	0.073	0.073	0.073	0.073	0.073	0.073	0.073	0.073	0.073		
0.25		0.073	0.072	0.059	0.073	0.071	0.073	0.073	0.073	0.073	0.073		
0.35				0.054	0.073	0.073	0.073	0.073	0.073	0.073	0.073	0.073	
0.45					0.073	0.073	0.073	0.073	0.073	0.073	0.073	0.073	
0.55						0.049	0.073	0.073	0.073	0.073	0.073		
0.65						0.053	0.073	0.073	0.073	0.073	0.073		
0.75							0.073	0.073	0.073	0.073	0.073	0.073	
0.85								0.073	0.073	0.073	0.073	0.073	
0.95								0.073	0.069		0.073	0.073	0.073
1.05								0.073	0.073	0.073		0.072	
1.15										0.073		0.073	
1.25													
1.35											0.058		

H_s [m]													
0.05	0.438	0.513	0.699	0.438	0.700	0.441	0.700	0.645	0.436	0.438	0.610	0.439	0.685
0.15		0.614	0.683	0.517	0.358	0.700	0.690	0.669	0.439	0.475	0.640		
0.25		0.700	0.700	0.700	0.520	0.700	0.326	0.542	0.699	0.543	0.514		
0.35				0.346	0.403	0.469	0.443	0.534	0.483	0.542	0.474	0.383	
0.45					0.393	0.316	0.510	0.407	0.676	0.485	0.439	0.509	
0.55						0.409	0.435	0.463	0.510	0.419	0.434		
0.65						0.347	0.638	0.376	0.540	0.524	0.410		
0.75							0.683	0.504	0.418	0.487	0.694	0.489	
0.85								0.515	0.378	0.311	0.541	0.668	
0.95								0.440	0.700		0.592	0.601	0.637
1.05								0.459	0.491	0.572		0.524	
1.15										0.700		0.582	
1.25													
1.35											0.463		

Figure 6: Optimized c_c (in Nms) and c_g (in 10^{-3} Nms) matrices for case 3.

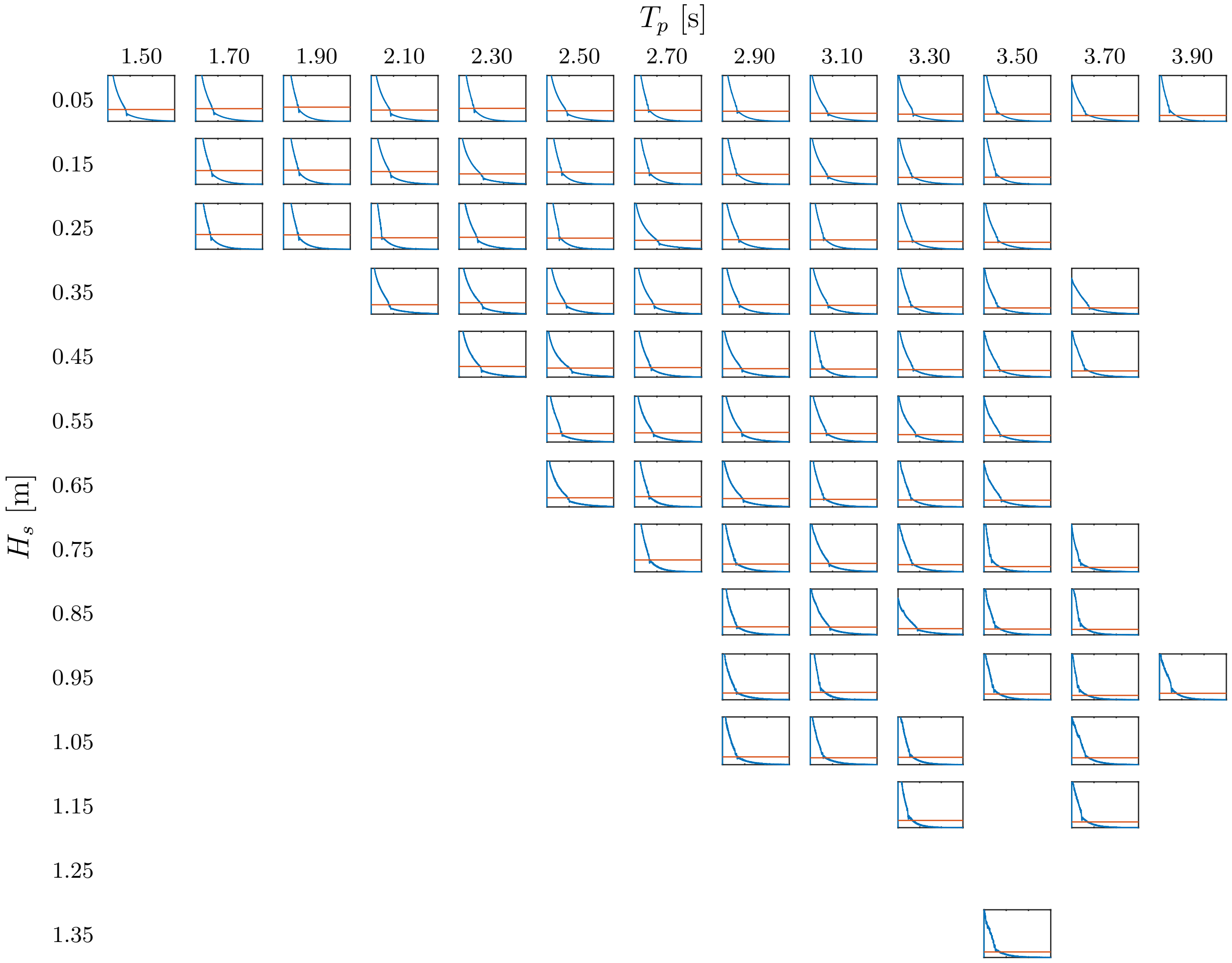

Figure 7: Instantaneous captured power for case 3, both c_c and c_g optimized.

3 Conclusion

The proposed magnetic coupling mechanism has not been found able to improve the stability (synchronization) of the GyroPTO in a realistic wave climate, i.e. Nissum Bredning. As seen from the simulation for the three cases, the absorbed power declines quite rapidly to zero no matter the choice of the control gains.

It appears that to improve the performance of the GyroPTO in irregular sea would require more sophisticated solutions. Some suggestions include properly changing the value of the generator gain in real time using a certain semi-active control law. Improving the performance of the current device is, however, likely to be challenging. Major modifications or completely new inventions integrated in a different setup could possibly be a better path to take, but it is not within the project's current scope of work to perform such investigations.

References

D. W. Gulick and O. M. O'Reilly. On the dynamics of the Dynabee. *Journal of Applied Mechanics*, 67(2):321–325, 2000.

Morten Mejlhede Kramer and Jens Peter Kofoed. Wave basin tests with Joltech's GyroPTO completed in March 2016. Technical Report 207, Department of Civil Engineering, Aalborg University, Denmark, 2016. (draft).

Morten Mejlhede Kramer, Arthur Francois Serge Pecher, Irene Guaraldi, Morten Thøtt Andersen, and Jens Peter Kofoed. Hydraulic evaluation of Joltech's GyroPTO for wave energy applications. Technical Report 178, Department of Civil Engineering, Aalborg University, Denmark, 2015.

K. Nielsen and T. Pontes. Annex II Task 1.1 Generic and site-related wave energy data. Technical Report T02-1.1, OES IA, September 2010.

Søren R. K. Nielsen, Zili Zhang, Morten M. Kramer, and Jan Olsen. Stability analysis of the gyroscopic power take-off wave energy point absorber. *Journal of Sound and Vibration*, 355: 418–433, 2015. doi:https://doi.org/10.1016/j.jsv.2015.06.029.

J. Olsen. Gyroelektrisk ansøgning, 2015. Project application to EUDP.

Zili Zhang, Bei Chen, Søren R.K. Nielsen, and Jan Olsen. Gyroscopic power take-off wave energy point absorber in irregular sea states. *Ocean Engineering*, 143:113–124, 2017. doi:http://dx.doi.org/10.1016/j.oceaneng.2017.07.050.

DCE Contract Report No. 194